

Received: 2019.01.07
Accepted: 2019.03.21
Published: 2019.04.13

A Novel Rat Model of Patellofemoral Osteoarthritis Due to Patella Baja, or Low-Lying Patella

Authors' Contribution:
Study Design A
Data Collection B
Statistical Analysis C
Data Interpretation D
Manuscript Preparation E
Literature Search F
Funds Collection G

ABCDEF 1 **Mingjian Bei**
ADEG 2 **Faming Tian**
BC 3 **Ning Liu**
BC 3 **Zhiyuan Zheng**
BC 3 **Xuehui Cao**
BC 2 **Hongfei Zhang**
BC 3 **Yudan Wang**
BD 3 **Yaping Xiao**
AD 1 **Muwei Dai**
AFG 1,4 **Liu Zhang**

1 Department of Orthopedic Surgery, Hebei Medical University, Shijiazhuang, Hebei, P.R. China
2 Meical Research Center, North China University of Science and Technology, Tangshan, Hebei, P.R. China
3 Department of Orthopedic Surgery, The Affiliated Hospital of North China University of Science and Technology, Tangshan, Hebei, P.R. China
4 Department of Orthopedic Surgery, Meitan General Hospital, Beijing, P.R. China

Corresponding Author: Liu Zhang, e-mail: zhliu130@sohu.com

Source of support: This study was supported by the National Natural Science Foundation of China (No.31671235; No.81874029), and the Major Program of Natural Science Foundation of Hebei Province Nature Science Foundation (No.H201609176)

Background: Patella baja, or patella infera, consists of a low-lying patella that results in a limited range of motion, joint pain, and crepitations. Patellofemoral joint osteoarthritis (PFJOA) is a subtype OA of the knee. This study aimed to develop a reproducible and reliable rat model of PFJOA.


Material/Methods: Three-month-old female Sprague-Dawley rats (n=24) included a baseline group (n=8) that were euthanized at the beginning of the study. The sham group (n=8), and the patella ligament shortening (PLS) group (n=8) were euthanized and evaluated at ten weeks. The PLS model group (n=8) underwent insertion of a Kirschner wire under the patella tendon to induce patella baja. At ten weeks, the sham group and the PLS group were compared using X-ray imaging, macroscopic appearance, histology, immunohistochemistry, TUNEL staining for apoptosis, and micro-computed tomography (micro-CT). The patella height was determined using the modified Insall-Salvati (MIS) ratio.

Results: The establishment of the rat model of patella baja in the PLS group at ten weeks was confirmed by X-ray. In the PLS group, patella volume, sagittal length, and cross-sectional area were significantly increased compared with the sham group. The PFJ showed typical lesions of OA, confirmed macroscopically and histologically. Compared with the sham group, in the rat model of PFJOA, there was increased cell apoptosis, and immunohistochemistry showed increased expression of biomarkers of osteoarthritis, compared with the sham group.

Conclusions: A rat model of PFJOA was developed that was confirmed by changes in cartilage and subchondral bone.

MeSH Keywords: **Cartilage • Models, Animal • Osteoarthritis, Knee • Patellofemoral Joint**

Full-text PDF: <https://www.medscimonit.com/abstract/index/idArt/915018>

 4796

 1

 9

 63



Background

Osteoarthritis (OA) is the most common chronic joint disease and affects more than 100 million people worldwide [1]. As the population ages and the rate of obesity increases, the prevalence of OA is projected to double by the year 2020 [2]. The knee joint is commonly affected OA and is a tricompartmental structure comprising the patellofemoral joint (PFJ) and medial and lateral tibiofemoral joints (TFJs). Previous studies of OA of the knee have focused on the TFJs, while the PFJ has rarely been studied. However, isolated patellofemoral joint osteoarthritis (PFJOA) is common and has a high prevalence in women (17.1–34.0%) and men (18.5–19.0%) more than 55–60 years old [3,4].

Patella baja, or patella infera, is a congenital or acquired low-lying patella that results in a limited range of motion (ROM), joint pain, and crepitations. Clinically, patella baja is a common cause of PFJOA and often occurs as a severe complication following knee surgery and trauma. Patella baja can result in patellar ligament shortening (PLS), fibrosis of Hoffa's fat pad, and other complications. There is a lack of data regarding the pathogenesis and mechanism of PFJOA, despite the important role that the PFJ plays in OA of the knee [5]. This finding may be because studies of PFJOA in humans are restricted by the slow rate of disease progression and the limited opportunities to investigate the tissue changes over time. Therefore, the study of animal models of PFJOA remains important for the understanding of approaches to clinical management.

Models of spontaneous PFJOA are characterized by slow disease progression, long study duration, and variable outcome [6–8]. Intra-articular administration of monosodium iodoacetate (MIA) in rats [9], which is considered to be a model of joint inflammation is caused by chemically-induced chondrocyte death, may not be a representative model of OA [10]. However, the MIA model has been primarily used for the study of pain associated with OA [11]. Surgically-induced models of OA models have been used mainly to study tibiofemoral joint osteoarthritis (TFJOA), and there have been few reported studies on PFJOA [12–14]. Also, previous animal models of PFJOA have included large animal and have involved major surgical procedures. The need for a new animal model of PFJOA in a small animal prompted the present study.

Therefore, this study aimed to establish a rat model of PFJOA induced by patella baja using PLS by minimally invasive surgery. The animal model was evaluated at multiple levels, using imaging, histology, and immunohistochemistry including the pathological changes in the cartilage, subchondral bone, and periarticular soft tissue.

Material and Methods

Animals

The experiments were performed on 3-month-old female Sprague-Dawley rats (249.0±6.5 g) (n=24) (Vital River Experimental Animal Technical Co., Ltd., Beijing, China). The rats were housed under standard 12-hour light and dark cycle, with *ad libitum* access to food and water. All experiments were conducted according to the Animal Research Reporting of *in Vivo* Experiments (ARRIVE) guidelines [15] and were approved by the institutional Animal Care and Use Committee (Approval No. 2017086).

Sprague-Dawley rats (n=24) included a baseline group (n=8) that were euthanized at the beginning of the study, after an X-ray examination. The sham group (n=8), and the patellar ligament shortening (PLS) group (n=8) were euthanized and evaluated at ten weeks. The sample size was determined by sample size calculations with a large effect size of Cohen's *d* (1.58) according to *a priori* power analysis based on bone mineral density (BMD) results (desired power=0.8; $\alpha=0.05$).

Surgery

The rats were anesthetized by intraperitoneal injection of pentobarbital, and knee surgery was performed (either PLS or sham surgery). Antibiotic prophylaxis with penicillin (150 IU/kg) was administered before and 3 days following surgery. For the performance of PLS, the skin was shaved and disinfected, and the right knee joint was exposed through a medial parapatellar approach with an approximately 1 cm incision from the patella to the tibial tuberosity. Care was taken to ensure that the patellar ligament was separated. A Kirschner wire measuring 7 mm in length and 2 mm diameter was used with 1-0 nylon sutures on the groove at 1 mm medial to both ends and was inserted under the patellar tendon from the medial to lateral region, and the sutures crossed each other at the proximal end of the patellar tendon. The sutures were then passed under both grooves, and the ligature in the patellar ligament was tightened with the knee in a position of maximum extension. Finally, the skin was closed with 3-0 nylon sutures (Figure 1). In the sham surgery rat group, the patellar ligament was left intact and only a skin incision was made, and then closed.

At 10 weeks postoperatively, all rats in each group underwent evaluation of patella baja by X-ray analysis under anesthesia. The rats were euthanized for macroscopic joint scoring, micro-computed tomography (micro-CT) scanning, and standard decalcification, paraffin-embedding and tissue sectioning for histological procedures.

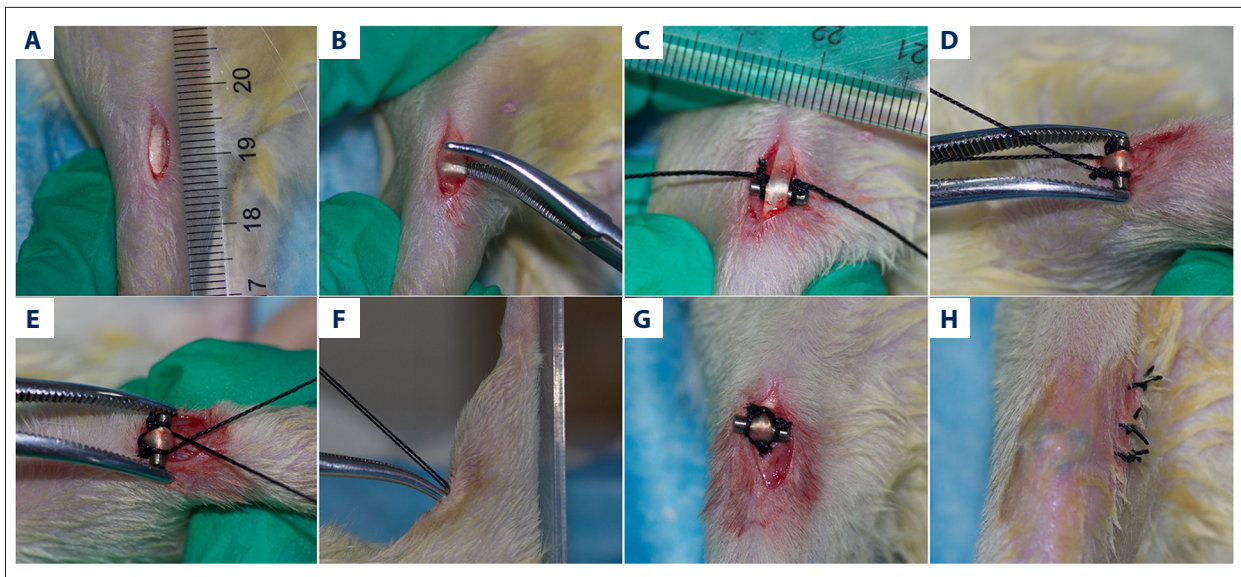


Figure 1. The surgical procedure of patellar ligament shortening (PLS) in the rat model of patellofemoral joint osteoarthritis (PFJOA). (A) The 1 cm longitudinal medial para-articular incision, performed after sterilizing the skin. (B) Blunt separation of the patella tendon. (C) Kirschner wire, 7 mm in length and 2 mm in diameter, with a groove with a 1-0 nylon suture at both ends at a distance of 1 mm, was inserted under the patella tendon from medial to lateral. (D) The sutures crossed each other at the proximal end of the patella tendon. (E-G) The sutures were passed under both grooves, and the ligature in the patella ligament was tightened with the knee in a position of maximum extension. (H) The skin was closed with 3-0 nylon sutures.

Radiography and manual palpation

The knees of the rats in the sham group and the PLS group were radiographed under general anesthesia. The rats were positioned in approximately 90° flexion with a specific right-angle device, and digital images of the knee joint were taken at 75 kV and 50 Hz using an Opera Swing X-radiography system (General Medical Merate, Via Partigiani, Seriate BG, Italy). Three independent observers measured and scored the images, according to the protocol previously described [16]. Figure 2Aa shows the method used to assess patellar height and the modified Insall-Salvati (MIS) ratio (g/f). Immediately after radiography, the rats were manually manipulated to move the Kirschner wire sideways and to determine the stabilization of the joint fixation.

Macroscopic findings

The rats in the sham group and the PLS group were killed after manual palpation. The femoral trochlea and patella of the right knee were photographed with a Canon 550D digital camera (Canon, Tokyo, Japan) and fixed in 10% formalin. Gross morphologic grading of the patella and trochlea was performed separately based on the scale previously described [17], and as follows: grade 0 (normal appearance); grade 1 (slight yellowish discoloration of the chondral surface); grade 2 (small cartilage erosions in load-bearing areas); grade 3 (large erosions extending down to the subchondral bone); and grade 4 (large erosions with exposure of large areas of subchondral bone).

Micro-computed tomography (micro-CT) imaging

To investigate the alterations in the subchondral bone micro-architecture, the patellofemoral joint (PFJ) was imaged using micro-computed tomography (micro-CT) with a SkyScan 1176 scanner (Bruker, Kontich, Belgium) with a resolution of 18 μm per voxel, after macroscopic analysis. Both regions of interest (ROIs) of the trochlea and patella were located under the subchondral bone plate at the cross-sectional level, excluding the cortical shell. The bone mineral density (BMD), bone volume to total volume fraction (BV/TV fraction), trabecular number, trabecular thickness, the trabecular separation, the structure model index, trabecular pattern factor, and degree of anisotropy were calculated. The sagittal length and cross-sectional area at different locations distant from the proximal patella were used to investigate the damage of the patellar structure.

Histology

In the rats, the right patellofemoral joints were harvested, cleaned of the soft tissues, fixed in 10% formalin, decalcified, dehydrated in a graded series of ethanols and embedded in paraffin wax according to standard protocols. The tissue blocks were then sectioned in the horizontal plane at 6 μm in thickness. Tissue sections were stained for light microscopy with hematoxylin and eosin (H&E) to evaluate the pathological changes in the synovium and infrapatellar fat pad, using the Osteoarthritis Research Society International (OARSI) score [10],

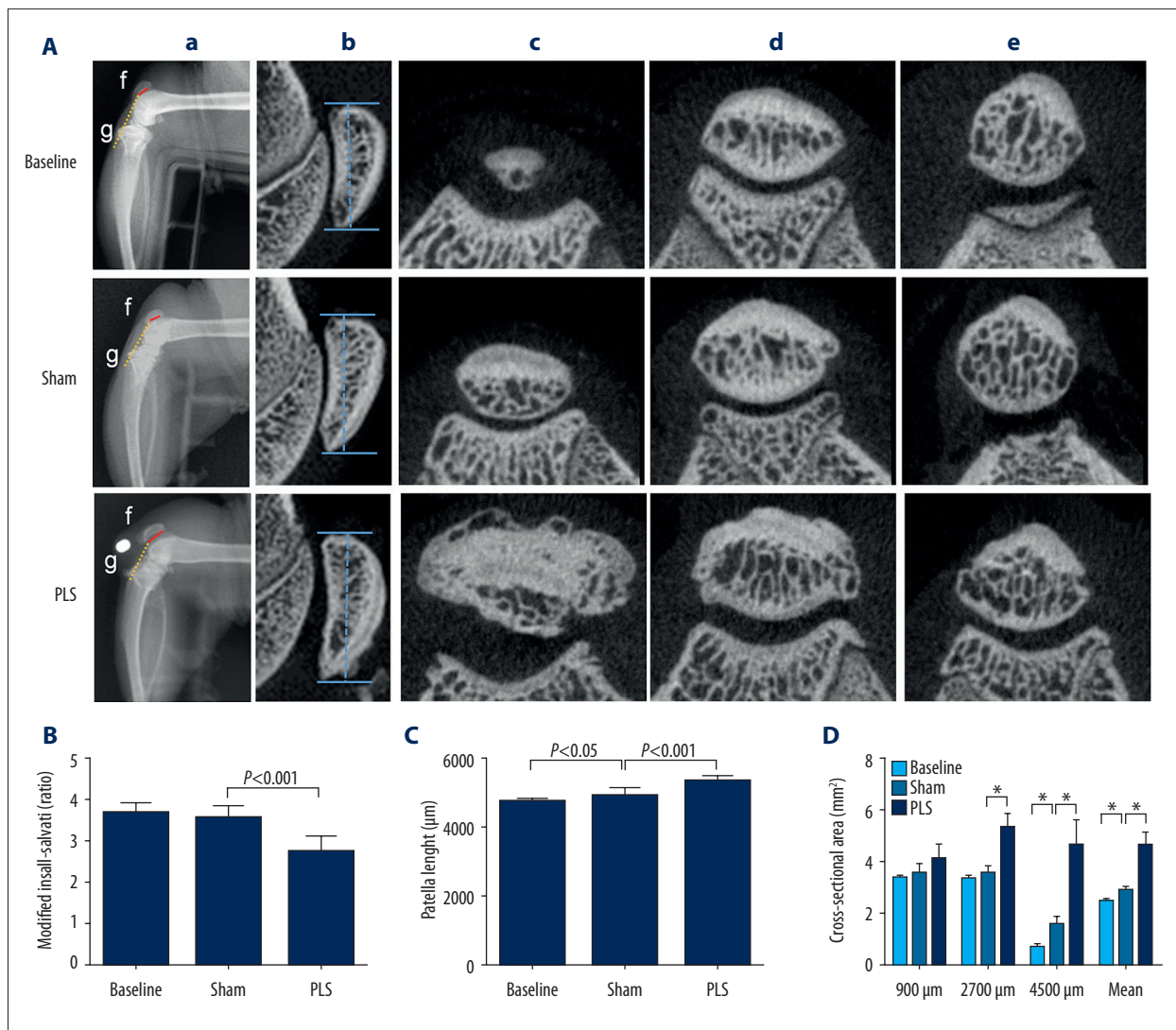


Figure 2. Imaging findings of the patella baja created by patellar ligament shortening (PLS) surgery in the rat model of patellofemoral joint osteoarthritis (PFJOA). **(A)** X-radiograph images of the patella baja and changes of patella structure induced by PLS surgery. **a)** Radiographies of the lateral right knee in approximately 90° flexion with a specific right-angle device. **b)** X-radiographs of the sagittal length of the patella. **c), d), e),** representative cross-sectional micro-computed tomography (micro-CT) images at 4500 µm, 2700 µm, and 900 µm distal from the proximal region of the patella, respectively. **f)** The length of the patellar articular surface. **g)** The distance from the inferior edge of the patella articular surface to the end of the patella tendon. **(B)** The modified Insall-Salvati (MIS) ratio. **(C)** The patella length. **(D)** The analysis of cross-sectional area at different locations distant from the proximal region of the patella. Data are expressed as the mean ± standard deviation (SD). * P<0.05 versus the baseline group. # P<0.05 versus the sham group.

and the percentage of the area that included adipose cells was determined. Cartilage degradation was assessed using Safranin O for glycosaminoglycans in cartilage and fast green counterstain for protein and scored using a semi-quantitative histopathological grading system based on OARSI score (Table 1) [18,19]. Six different ROIs of the articular cartilage, including both the load-bearing and non-load-bearing areas of the trochlea and patella, were scored and summed to give a maximum possible score of 36.

Immunohistochemistry

Immunohistochemistry was performed with primary antibodies to collagen type II (COL2A1) (1: 100) (DSHB Hybridoma Product II-II6B3, from Linsenmayer TF), matrix metalloproteinase-3 (MMP-3) (1: 100) (Bioss Inc., Beijing, China), signal transducer and activator of transcription 3 (STAT3) (1: 200) (Proteintech, Wuhan, China), cathepsin K (1: 100) (Affinity Bioscience, OH, USA), and osteoprotegerin (OPG) (1: 200) (Abcam, Cambridge, UK). Briefly, deparaffinized tissue sections

Table 1. The Osteoarthritis Research Society International (OARSI) semi-quantitative scoring system for osteoarthritic change.

Score	Key feature
0	Normal
0.5	Loss of Safranin O staining without structural changes
1	Small fibrils without loss of cartilage
2	Vertical clefts down to the layer immediately below the superficial layer and some loss of surface lamina
3	Vertical clefts/erosions in the calcified cartilage involving <25% of the articular surface
4	Vertical clefts/erosion in the calcified cartilage involving 25–50% of the articular surface
5	Vertical clefts/erosion to the calcified cartilage involving 50–75% of the articular surface
6	Vertical clefts/erosion to the calcified cartilage involving >75% of the articular surface

were rehydrated with ethanol, digested with 0.05% trypsin, treated with 3% hydrogen peroxide, and incubated with the primary antibodies overnight at 4°C. Immunohistochemistry was performed according to the instructions provided by the PV-6000 Polink-1 horse-radish peroxidase (HRP) DAB Detection System (ZSGB-Bio Corp., Beijing, China) and the ZLI-9018 DAB kit (ZSGB-Bio Corp., Beijing, China). Finally, the slides were counterstained with hematoxylin. The results were expressed as an average intensity of optical density (IOD/mm²), according to the method previously described [20,21].

TUNEL staining

The ApopTag® Peroxidase *in Situ* Apoptosis Detection Kit (Merck Millipore, Burlington, MA, USA) was used to detect apoptotic chondrocytes in cartilage, according to the manufacturer's instructions. The apoptotic cells were evaluated as the percentage of TUNEL-positive cells in the cartilage by using ImageJ software (National Institutes of Health, Bethesda, MD, USA), as previously described [22].

Statistical analysis

All data were presented as the mean ± standard deviation (SD), with the exception of the macroscopic and histological data, which were presented as the median and interquartile range (IQR). One-way analysis of variance (ANOVA) followed by Fisher's least significant difference (LSD) t-test or Dunnett's T3 test were used for pairwise comparison of data with a Gaussian distribution and homogeneity of variance. Kruskal-Wallis and Mann-Whitney non-parametric analysis were used for non-Gaussian distributed data, as appropriate. The level of statistical significance was established at P<0.05. Statistical analysis of data was performed using SPSS version 19.0 (SPSS Inc. Chicago, IL, USA).

Results

The rats in the sham group (n=8), and the patellar ligament shortening (PLS) group (n=8) responded well to anesthesia and showed signs of swelling, limping, and limb withdrawal at 72 h postoperatively. No difference in the walking pattern was found in the sham group and PLS group after one week postoperatively. None of the rats showed signs of bacterial infection in the knee and no rats died during the experimental period.

Assessment of radiographic findings and Kirschner wire position

As shown in Figure 2Aa, according to the radiographic evaluation and manual palpation, the Kirschner wire provided stable fixation with no detachment. The rats in the PLS group showed a significantly lower position of the patella, as evaluated using the modified Insall-Salvati (MIS) ratio (MIS ratio, 2.76±0.34) compared with the sham group (MIS ratio, 3.59±0.28; P<0.001) and with the baseline group (MIS ratio, 3.68±0.24; P<0.001). The MIS ratio was not significantly different between the baseline group and the sham rat group (P>0.05) (Figure 2B).

Patellar structure

Changes in the patellar structure were investigated in the rat model, as shown in Figure 2Ab–e. The sham group also showed a significantly shorter sagittal length of the patella compared with the PLS group (P<0.001), which was significantly longer than the baseline group (P<0.05) (Figure 2C). The cross-sectional area of the patella was significantly smaller in the sham group compared with the PLS group (P<0.001 for 2700 μm, 4500 μm, and the mean), and significantly larger than the baseline group (P<0.001 for 4500 μm and mean) (Figure 2D).

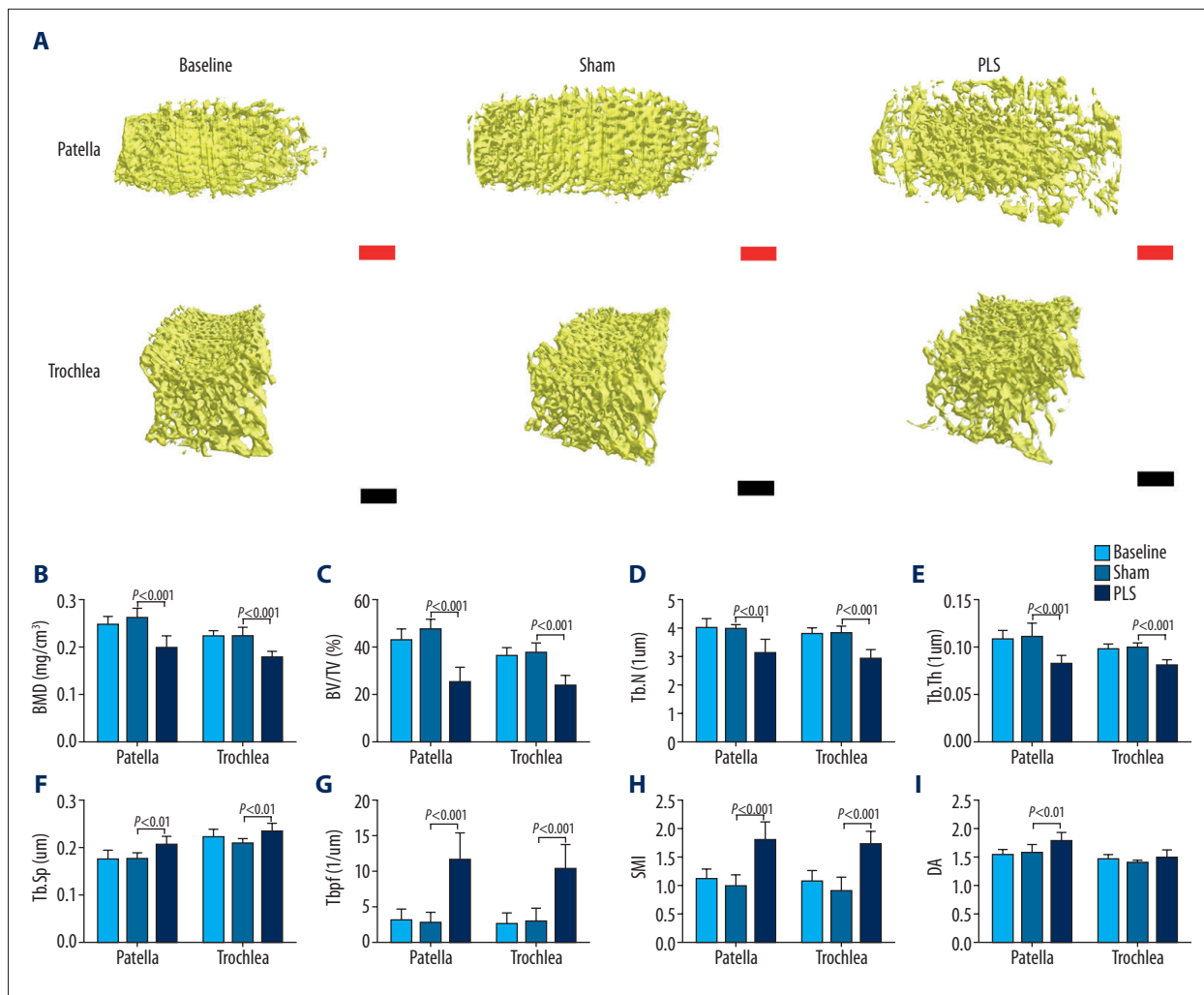


Figure 3. The pathological and structural changes in the subchondral bone of both the patella and trochlea induced by patellar ligament shortening (PLS) surgery in the rat model of patellofemoral joint osteoarthritis (PFJOA). (A) The pathological changes in the subchondral bone of both the patella and trochlea induced by patella ligament shortening (PLS) surgery. (B) Micro-computed tomography (micro-CT) analysis of the trabecular bone mineral density (BMD). (C) Bone volume fraction, or bone volume (BV)/total volume (TV). (D) Trabecular number (Tb.N). (E) Trabecular thickness (Tb.Th). (F) Trabecular separation distance (Tb.Sp). (G) Trabecular pattern factor (Tb.pf). (H) Structure model index (SMI). (I) The degree of anisotropy (DA). Red bars=100 μm. Black bars=250 μm. Data are expressed as the mean ± standard deviation (SD).

Micro-computed tomography (micro-CT) measurement of subchondral bone

Three-dimensional reconstructed images of the subchondral bone of both the patella and trochlea are shown in Figure 3A. The results showed a significant decrease in the bone mineral density (BMD) ($P < 0.001$ for both), bone volume to total volume (BV/TV) fraction ($P < 0.001$ for both), trabecular number ($P < 0.01$ for the patella; $P < 0.001$ for the trochlea), and the trabecular thickness ($P < 0.001$ for both), a significantly increased trabecular separation ($P < 0.01$ for both), degree of anisotropy ($P < 0.01$ for the patella), the trabecular pattern factor ($P < 0.001$ for both), and structure model index ($P < 0.001$ for both) in the

PLS group compared with the sham group. There was no significant difference in the results between the baseline and the sham rats ($P > 0.05$ for both) (Figure 3B–I).

Macroscopic findings of cartilage lesions

In the macroscopic findings, as shown in Figure 4A, the cartilage of the joints in the baseline and sham groups showed no cartilage erosion and had smooth glistening surfaces. In contrast, the cartilage in the rats with PLS-induced osteoarthritis (OA) showed a rough articular surface and marked cartilage erosion, which was more severe in the weight-bearing areas of the trochlea and at the inferior pole of the patella.

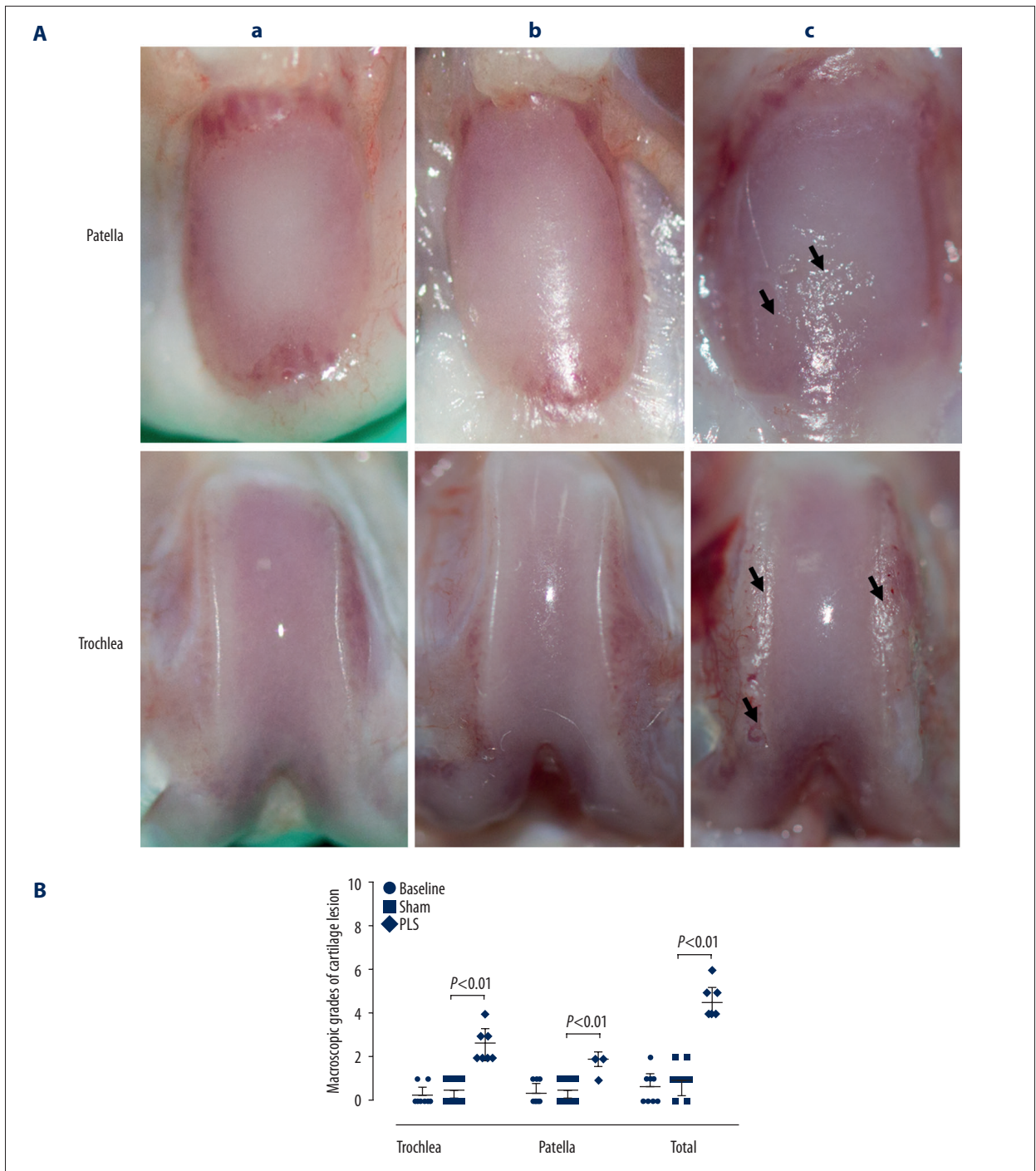


Figure 4. The macroscopic images and scores in the patella and trochlea induced by patellar ligament shortening (PLS) surgery in the rat model of patellofemoral joint osteoarthritis (PFJOA). The macroscopic images (A) and scores (B) of injury in the patella and trochlea. **a**) The baseline group (n=8). **b**) The sham group (n=8). **c**) The patella ligament shortening (PLS) group (n=8). The macroscopic images of the cartilage surface of both the patella and trochlea in the rats that underwent PLS surgery-induced patella baja showed cartilage erosion when compared with normal cartilage in the sham group. Black arrows indicate large cartilage erosion. Data are expressed as the median and interquartile range (IQR).

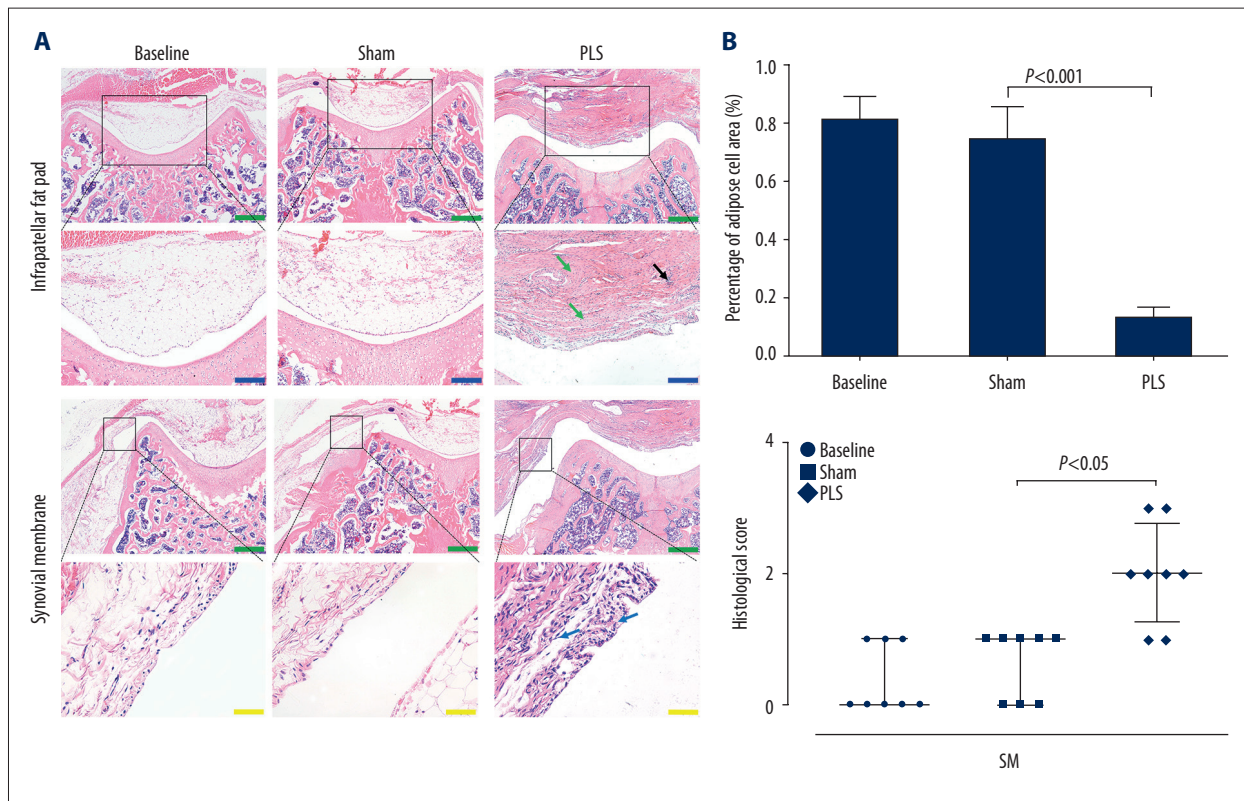


Figure 5. Photomicrographs of the histology of the patella and trochlea induced by patellar ligament shortening (PLS) surgery in the rat model of patellofemoral joint osteoarthritis (PFJOA). **(A)** Representative histological images of the infrapatellar fat pad (IFP) and synovial membrane (SM). Hematoxylin and eosin (H&E). **(B)** Analysis of the histological results of the infrapatellar fat pad (IFP) and synovial membrane (SM), respectively. The black arrow indicates the loss of adipocytes with an inflammatory cell infiltration. The green arrow indicates fibroplasia. The blue arrow indicates synovial cell proliferation. Blue bars=200 μ m. Green bars=500 μ m. Yellow bars=50 μ m. Data are expressed as the mean \pm standard deviation (SD), with the exception of the scores of the synovial membrane (SM), which are presented as the median and interquartile range (IQR).

The macroscopic scores of the trochlea, patella in total were significantly higher in the PLS group compared with the sham group (all $P < 0.01$). Also, the baseline group scores did not differ significantly when compared with the sham group (all $P > 0.05$) (Figure 4B).

Histology, immunohistochemistry, and apoptosis of cartilage tissues

Light microscopy of the tissue sections stained with hematoxylin and eosin (H&E), Safranin O for glycosaminoglycans in cartilage, and fast green counterstain for protein showed typical destruction of the soft tissues and cartilage in the patellofemoral joint (PFJ), consistent with OA. Light microscopy with H&E staining showed synovial hyperplasia with a chronic inflammatory cell infiltrate with few lymphocytes. The same trend was found in the infrapatellar fat pad, which was characterized by necrosis and loss of adipocytes and widespread fibroplasia (Figure 5A). The findings in both the synovium and infrapatellar fat pad were more severe in the PLS group compared with

the sham group ($P < 0.05$ for the synovium; $P < 0.001$ for the infrapatellar fat pad), and no significant difference was seen between the baseline and the sham groups (all $P > 0.05$) (Figure 5B).

Safranin O and fast green histochemical staining showed irregularity of the surface of the articular cartilage with significant injury, which was more severe in the load-bearing regions of the trochlea and all regions of the patella in the PLS rat group. Also, patellar cartilage injury was present, including cartilage fibrils, chondrocyte swelling, horizontal clefts and denudation. Trochlear cartilage injury was characterized by large areas of erosion with fibrous tissue proliferation and chondrocyte clones in the load-bearing regions, while the non-load-bearing areas of the trochlea mainly showed irregularity of the surface of the articular cartilage. The tissue in the sham group appeared normal with only a slight decrease in Safranin O staining (Figure 6A). The Osteoarthritis Research Society International (OARSI) score in all regions of the patella and trochlea, including weight-bearing and non-weight-bearing regions, were significantly increased in the PLS group

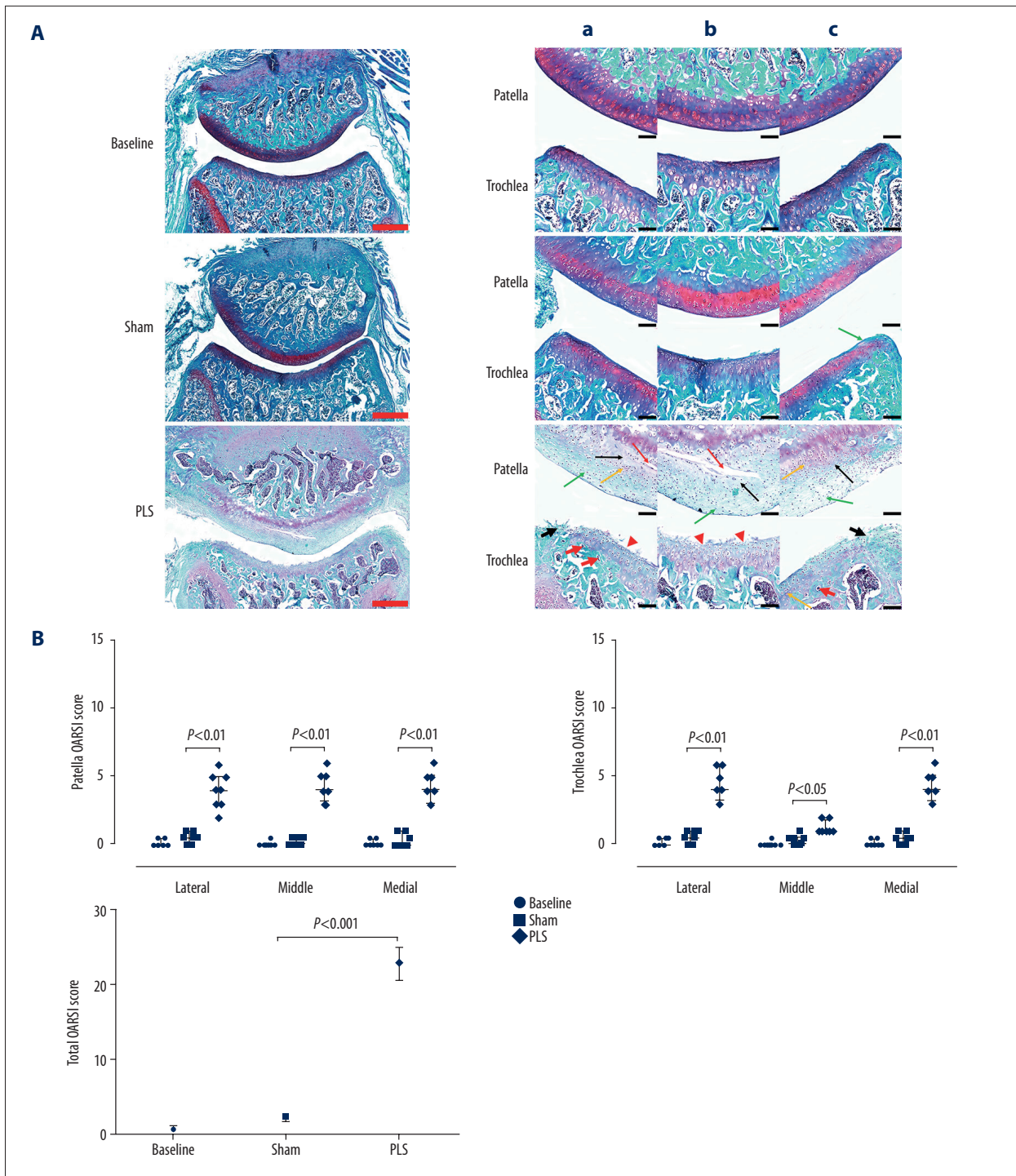


Figure 6. Photomicrographs of the histology of the patella and trochlea induced by patellar ligament shortening (PLS) surgery in the rat model of patellofemoral joint osteoarthritis (PFJOA). **(A)** Representative histological sections stained with Safranin O/fast green of the patellofemoral joint (PFJ) in the three rat study groups. Bilateral weight-bearing areas (**a**, lateral; **c**, medial) and non-weight-bearing areas (**b**) of the patella and trochlea. **(B)** Analysis of the Osteoarthritis Research Society International (OARSI) score of the patella, trochlea, and both, respectively. The green arrow indicates reduced Safranin O staining. The red arrow indicates horizontal clefts and denudation. The black arrow indicates cartilage swelling. The yellow arrow indicates chondrocyte clones. The red arrowhead indicates irregularities in the cartilage surface. The short black arrow indicates a large erosion with fibrous tissue proliferation. Red bars=500 μ m. Black bars=100 μ m. Data are expressed as the median and interquartile range (IQR).

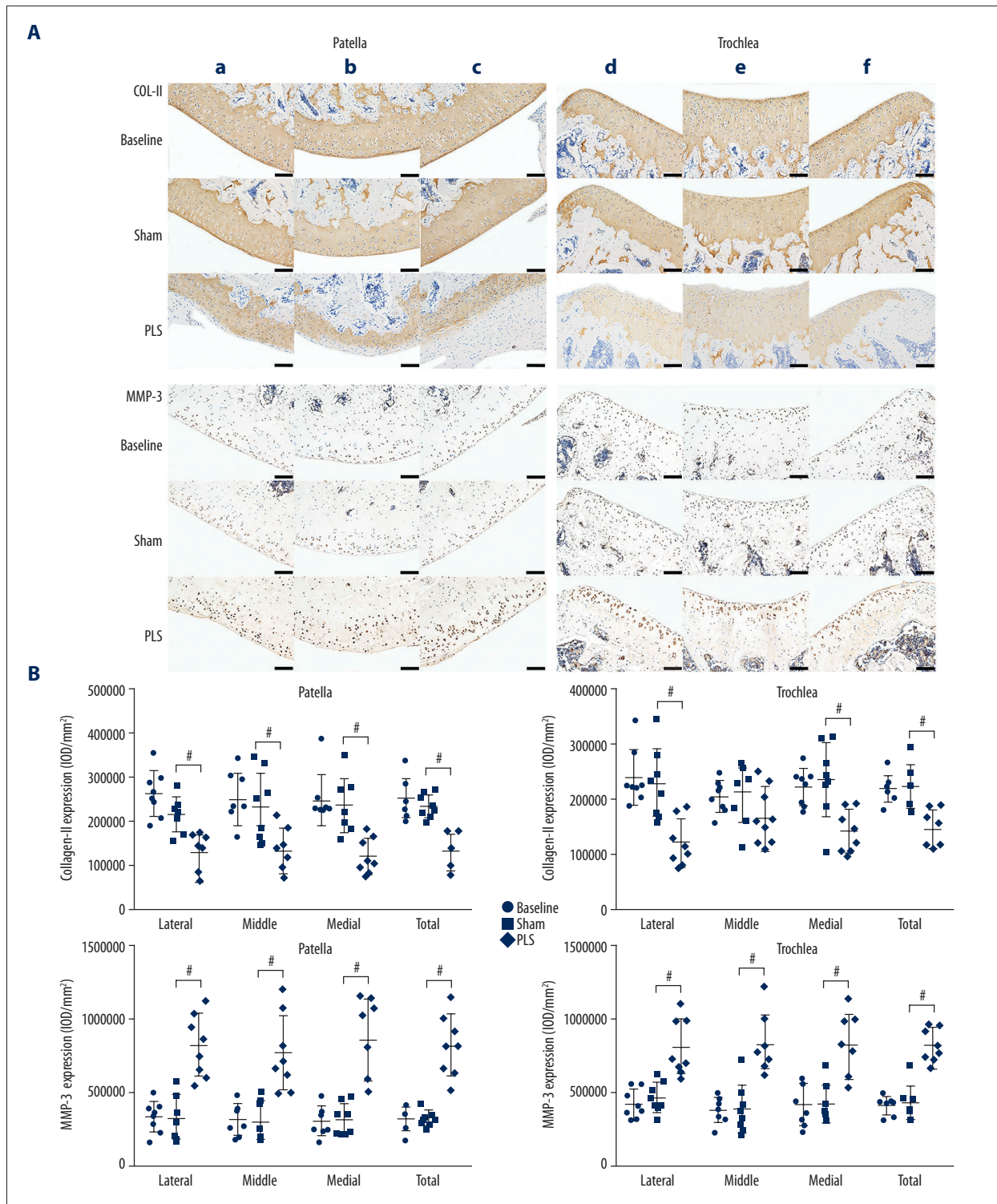


Figure 7. Photomicrographs of the immunohistochemistry of the patella and trochlea induced by patellar ligament shortening (PLS) surgery in the rat model of patellofemoral joint osteoarthritis (PFJOA). **(A)** Immunohistochemistry staining for collagen type II (COL2A1) and matrix metalloproteinase-3 (MMP-3) expression in the bilateral weight-bearing areas (**a, d**, lateral; **c, f**, medial) and non-weight-bearing areas (**b, e**) of cartilage in the patella and trochlea among the groups. **(B)** Quantification of protein expression of COL2A1 and MMP-3 in the patella and trochlea, respectively. Bars=100 μ m. Data are expressed as the mean \pm standard deviation (SD). $P < 0.05$ versus the sham group.

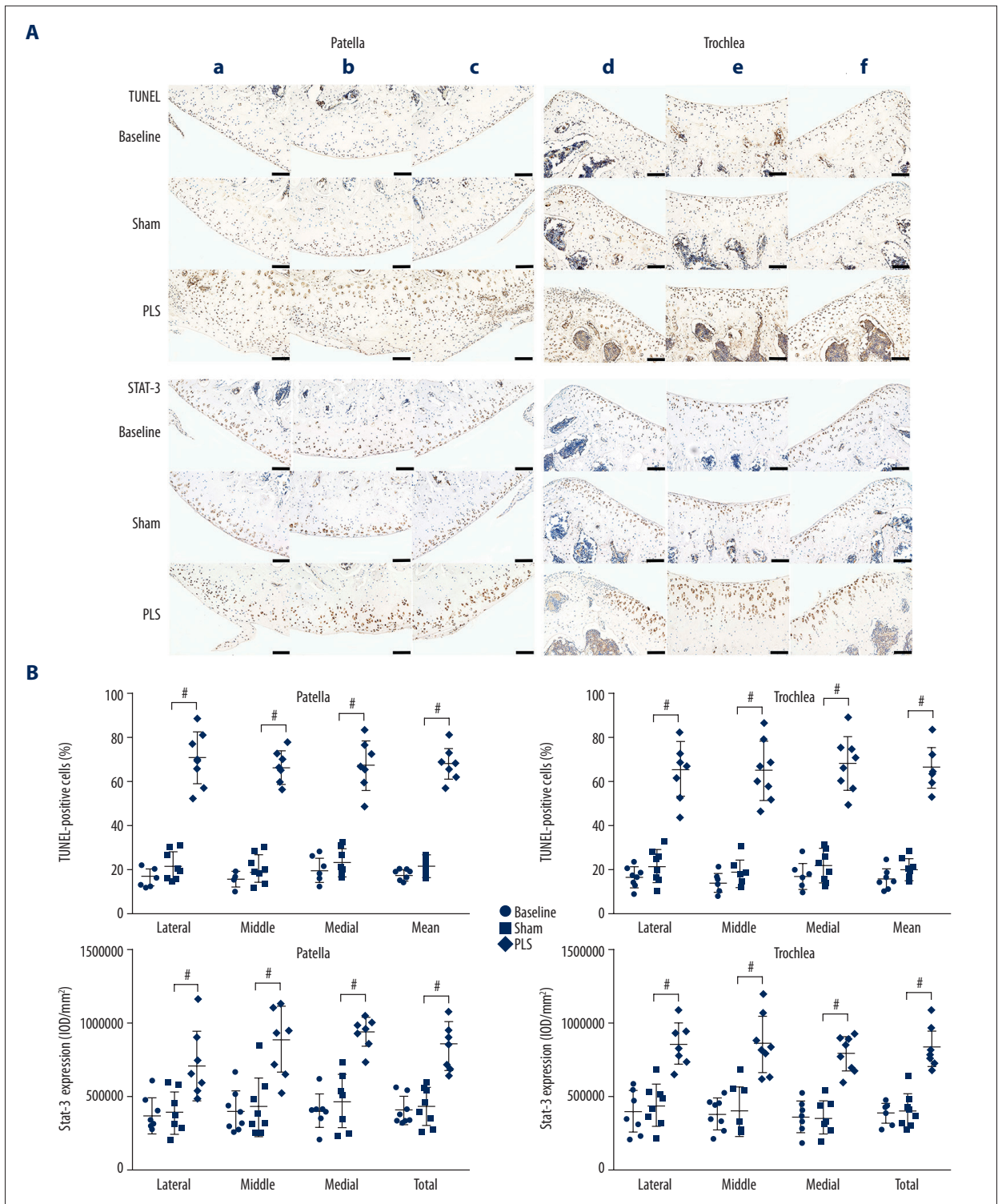


Figure 8. Photomicrographs of the TUNEL staining for cell apoptosis and immunohistochemistry for STAT3 of the patella and trochlea induced by patellar ligament shortening (PLS) surgery in the rat model of patellofemoral joint osteoarthritis (PFJOA). **(A)** Images of both the TUNEL staining and immunohistochemistry for STAT3 expression in the bilateral weight-bearing areas (a, d, lateral; c, f, medial) and non-weight-bearing areas (b, e) of cartilage in the patella and trochlea in the rat groups. **(B)** The quantified percentage of TUNEL-positive chondrocytes and protein levels of STAT3 in the patella and trochlea, respectively. Bars=100 μ m. Data are expressed as the mean \pm standard deviation (SD).# P<0.05 versus the sham group.

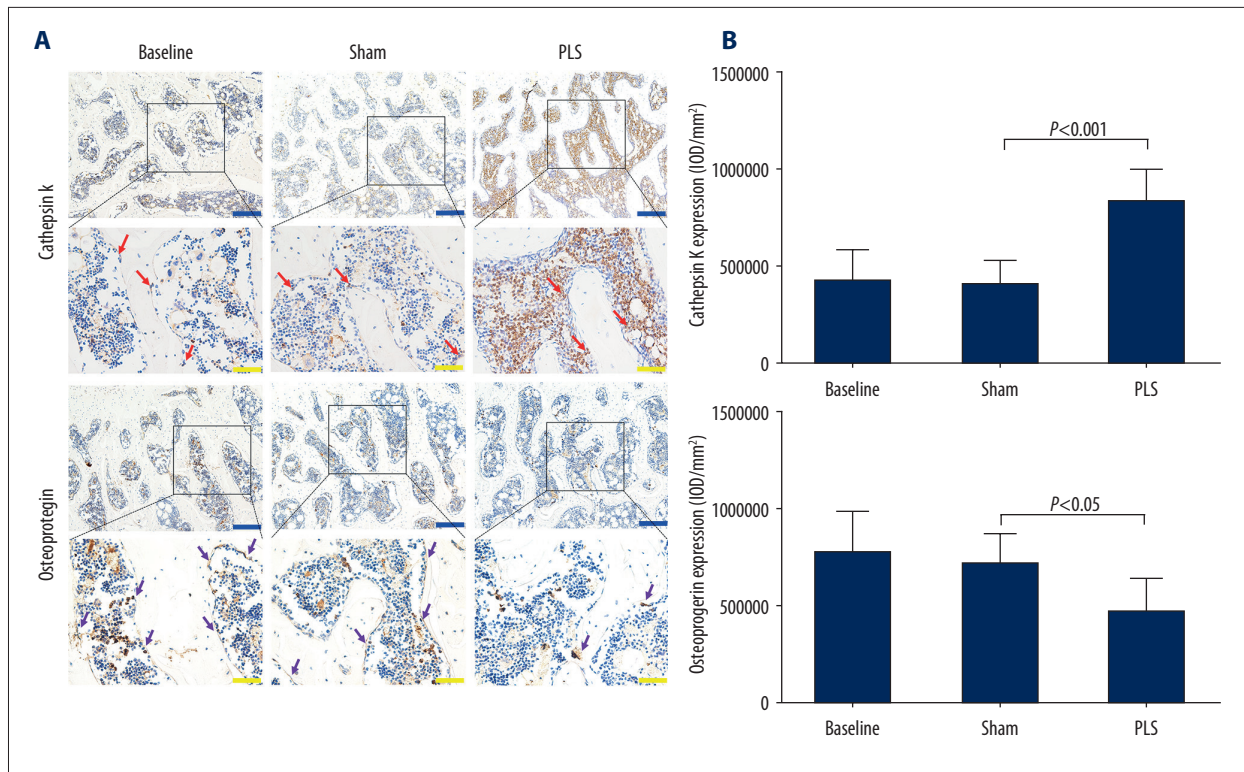


Figure 9. Photomicrographs of the immunohistochemistry for cathepsin K and osteoprotegerin (OPG) of the patella and trochlea induced by patellar ligament shortening (PLS) surgery in the rat model of patellofemoral joint osteoarthritis (PFJOA). **(A)** Representative immunohistochemical images of both cathepsin K and osteoprotegerin (OPG) in the subchondral bone. **(B)** The quantified protein levels of cathepsin K and OPG in the subchondral bone. The red arrow indicates the expression of cathepsin K-positive-stained cells. The purple arrow indicates the expression of OPG-positive cells. Blue bars=200 μ m. Yellow bars=50 μ m. Data are expressed as the mean \pm standard deviation (SD).

compared with the sham group (all $P < 0.05$), and no significant difference was seen between the baseline group and the sham group (all $P > 0.05$) (Figure 6B).

Molecular changes that regulate the metabolism and apoptosis of the chondrocytes in cartilage at the molecular level were present in this rat model (Figures 7, 8A). Compared with the protein expression in the patella and trochlea in the sham group, collagen II as the main matrix component, was significantly down-regulated in the PLS group (both $P < 0.05$ for all but for the middle region of the trochlea). In contrast, the matrix-degrading protease, matrix metalloproteinase 3 (MMP-3) was upregulated in the PLS group and was mainly expressed in the chondrocytes adjacent to the lesions (both $P < 0.01$, for all regions) (Figure 7B). The expression of STAT3 was significantly increased in the PLS rat model compared with the sham rats. Also, TUNEL staining showed a larger number of apoptotic chondrocytes in cartilage in the PLS group compared with the sham group (both $P < 0.001$ for all regions) (Figure 8B). The results of these indicators did not differ significantly between the sham group and the baseline group (all $P > 0.05$ for all regions) (Figures 7, 8B).

To further understand the molecular events underlying the destruction of the subchondral bone following PLS surgery, the expression of cathepsin K and osteoprotegerin (OPG) in the subchondral bone was evaluated (Figure 9A). The expression of cathepsin K-positive cells was significantly reduced, whereas the expression of OPG was significantly increased in the sham group compared with the rats in the PLS group ($P < 0.01$), and did not reach statistical significance when compared with rats in the baseline group ($P > 0.05$) (Figure 9B). These findings indicated that the activity of osteoclasts increased in rats in the PLS group.

Discussion

In this study, multiple approaches were used to evaluate a new rat model of patellofemoral joint osteoarthritis (PFJOA) that was successfully established by inducing patella baja using patellar ligament shortening (PLS). First, radiographic imaging and calculation of the modified Insall-Salvati (MIS) ratio supported that this approach successfully established a patella baja model. Second, the histological findings showed that patella

baja induced the formation of typical osteoarthritis (OA) lesions in the patellofemoral joint (PFJ), including degenerative changes in the articular cartilage of the patella and trochlea, synovitis, and fibrosis of the infrapatellar fat pad. Third, immunohistochemistry demonstrated an imbalance between the anabolism and catabolism of cartilage with increasing of osteoclast activity and decreasing of osteoblast activity in the subchondral bone, and apoptotic chondrocytes were demonstrated by TUNEL staining. Finally, micro-computed tomography (micro-CT) confirmed deterioration of the microarchitecture of the trabecular bone, which is a feature of early OA, and alterations of the patellar structure in cross-sectional area and length. To the best of our knowledge, this is the first study to demonstrate that PLS can effectively induce OA-like lesions in the PFJ in a rodent model.

There have been previously described animal models of PFJOA. The most thoroughly characterized animal models involving PFJOA is the anterior cruciate ligament transection model in cats [12,14], rabbits [13], and rats [23]. Other surgical models involve changes to muscle strength [24,25] and realignment of the patella [26]. Although these surgical models induced the occurrence of PFJOA, the process destroyed the integrity of the joint capsule and exposed the joint cavity. Spontaneous PFJOA models are characterized by a slow disease process with a longer study period and more variable outcome [6–8]. Although intra-articular injection of monosodium iodoacetate (MIA) could induce the onset of the PFJOA in rats [9], which is considered to be a model of cartilage damage, aggressive subchondral bone lesions, and inflammation is caused by chemically-induced chondrocyte death rather than a model of OA that is typical of the disease [10], and have been primarily used to investigate behaviors related to OA-induced pain [11].

Currently, there is no ideal animal model for OA that considers the differences in size, anatomy, histology, biochemical parameters, and physiology between animals and humans [27,28]. In the present study, we established a low-cost small animal model that exhibited changes similar to a degenerative PFJ using a relatively less invasive manipulation without exposing the joint cavity. However, this study had several limitations. First, because the PFJOA model was established using rats, the animal was smaller and less comparable with human than larger animal models, especially with respect to the composition of the cartilage [8]. Second, the rapid course of PFJOA in this model made it less responsive to interventions than spontaneous OA models [29], in contrast to the natural course of OA in humans, which is characterized by slow disease progression. Third, data were lacking regarding patella baja at different time points, and this will be the subject of future studies. However, data from cartilage and subchondral bone at both the tissue and molecular levels have established a reference for future studies using this animal model.

In this study, the histological scores demonstrated that cartilage degradation with synovitis and fibrosis of the infrapatellar fat pad were evident in the PLS rat group, which were findings supported by those from a previous study [9]. The damage to patellar cartilage in the present study was characterized by the formation of cartilage fibrils, swelling, horizontal clefts, and denudation. Large areas of cartilage erosion were seen in the weight-bearing areas of the trochlea, with fibrous tissue proliferation, which were histological findings supported by published clinical studies in PFJOA [30–32]. Previous studies of the effect of PLS on the PFJ have focused on the patellofemoral alignment [33], and kinematics [34,35]. Histological changes in matrix staining and damage to the subchondral bone of the PFJ have seldom been previously evaluated. Also, the present study showed marked synovial inflammation and infrapatellar fat pad fibrosis with thickening of the synovial cell layers and loss of adipocytes separated by fibrous tissues following PLS. The previous studies by Bondeson et al. and Clockaerts et al. showed that inflammation of the synovium and the infrapatellar fat pad might play a role in OA of the knee [36,37]. The findings of the present study were similar to previously published findings in post-traumatic OA, in that these changes facilitated the development of cartilage damage [38,39]. The findings of the present study complement the current literature on what is known of the effect of PLS on the PFJ.

To investigate the mechanism underlying damage to the joint cartilage in the protocol for the development of this animal model, metabolism and apoptosis of cartilage were assessed, as these are important factors in the pathogenesis of OA. The findings from the immunohistochemistry and TUNEL staining showed the presence of chondrocyte apoptosis, increased expression of matrix metalloproteinase-3 (MMP-3) and signal transducer and activator of transcription 3 (STAT3), and reduced expression of collagen type II (COL2A1), which were consistent with the presence of OA. Type II collagen is the major component of articular cartilage, and the loss of expression is a characteristic of OA [40]. MMP-3 has been shown to play a crucial role in cartilage destruction by activating other MMPs and degrading extracellular matrix [41]. Expression of the catabolic protein MMP-3 was increased, whereas expression of the anabolic protein collagen II was decreased in the present study. These findings were supported by those of Akhtar et al., who showed increased expression of MMP-3 mRNA but reduced expression of collagen II mRNA in a model of post-traumatic OA [42]. Cartilage degeneration also results from chondrocyte apoptosis, and in the present study, TUNEL-positive cells were significantly increased in the rat model of PFJOA. This finding is supported by the findings from Zhang et al. in a study that showed that apoptotic chondrocytes were significantly increased in cartilage in OA [43].

STAT proteins are involved in mediating cellular responses to cytokines [44]. Recently, Liu et al. and Latourte et al. demonstrated activation of the STAT3 pathway in human chondrocytes and destabilization of the medial meniscus in a mouse model of OA [45,46]. The phosphorylated STAT3 (phospho-STAT3)-positive chondrocytes increased six weeks after destabilization of the medial meniscus (DMM), and administration of Stattic, an inhibitor of STAT3, significantly inhibited IL-6-induced chondrocyte apoptosis and phosphorylation of STAT3 in chondrocytes when compared with controls [46]. The present study also showed that the STAT3 increased 10 weeks after PLS, which is similar to the findings reported by Latourte et al. [46]. Also, activation of the STAT3 pathway mediates increased expression of MMPs, including MMP-1, MMP-3, and MMP-13 in chondrocytes [47,48]. Therefore, it may be proposed that the activation of STAT3 in cartilage in the patella baja-induced PFJOA rat model may be involved in the upregulation of MMP-3 expression and chondrocyte apoptosis, resulting in catabolic metabolism of cartilage found in this model.

A strength of the present study was the degree of detail regarding the evaluation of the changes present in subchondral bone. Micro-computed tomography (micro-CT) analysis showed marked deterioration of the microstructure of the subchondral bone in PLS rats, characterized by a significantly lower bone mineral density (BMD), bone volume to total volume (BV/TV) fraction, the trabecular number, and the trabecular thickness and a significantly increased trabecular separation, degree of anisotropy, trabecular pattern factor, and structure model index compared with the sham rats. Burr et al. and Hayami et al. previously showed that subchondral bone abnormalities were present in the early stage of OA with high bone turnover and subsequent loss of bone mass [49,50], and the subchondral bone microstructure was destroyed with cartilage destruction [51]. These findings suggest that subchondral bone plays a critical role in the progression of OA.

In the present study, it was further demonstrated that osteoclast expression was increased in PLS rats by immunohistochemical detection of the osteoclast marker, cathepsin K [52]. The findings from the present study are supported by those of Liu et al. [53], who found that tartrate-resistant acid phosphatase (TRAP)-positive cells were enhanced in an animal model fed a large diet due to abnormal load on the temporomandibular joint (TMJ). Also, the expression of osteoprotegerin (OPG) was significantly reduced in the PLS rat group, which was a finding supported by Yang et al. who showed that reduced expression of OPG mRNA in a model of chemically-induced OA [54]. As a glycoprotein secreted by osteoblasts, OPG expression in osteoblasts blocks osteoclastogenesis and reduces mature osteoclast activity [55]. In the present study, the rats in the PLS group showed bone loss and deterioration in trabecular bone, which may be attributed to enhanced osteoclast activity and

reduced osteoblast activity caused by abnormal stress, and bone may adapt more rapidly than cartilage in response to altered mechanical stress [56]. Also, loss of trabecular bone may exert abnormal stress on the articular cartilage, and this change in the mechanics may initiate OA by destroying the physical integrity of the cartilage or altering cartilage metabolism [57].

Although the present study did not include quantitative analysis of osteophytes, a previous clinical study showed that the increased bone area in the medial and lateral compartments in TFJOA occurred in parallel with the increased grade of osteophytes [58]. The findings of the present study confirmed that the cross-sectional area and the patellar length in the sham rat group were significantly greater after 10 weeks of growth compared with the rats in the baseline group. There were similar findings in the rats in the PLS group when compared with rats in the sham group, which might be explained by two mechanisms. First, abnormal biomechanical traction followed by PLS might trigger an alteration in the patellar structure in the sagittal plane. Second, the further bone loss might reduce patellar skeletal adaptations and stimulate the growth of osteophytes, and the abnormal loads caused by patella baja might initiate the structural damage in the horizontal plane.

The radiographic results in this study demonstrated that patella baja was successfully induced by PLS in the rat model. The pathogenesis of PFJOA is linked to abnormal patellar kinematics, which catalyzes its initiation. Patella baja is defined as a short patellar tendon and is often caused by complex regional pain syndrome [59], trauma, immobilization or surgical procedures such as an opening wedge high tibial osteotomy [60]. Patellar misalignment caused by patella baja changes the patellofemoral contact pressure, increasing the joint reactive forces on both the patella and trochlea. Such abnormal loads may initiate the structural damage associated with PFJOA [61]. However, the intra-articular pressure was not measured in the present study, and although the patellar height can be evaluated on radiographs with numerous methods, no method is regarded as the gold standard [62]. The rats in this animal model were positioned with approximately 90° knee flexion to radiographically assess the patellar height, which differed from that in clinical radiographs taken to assess the patellar height at approximately 30° flexion of the standard weight-bearing lateral knee. The MIS ratio was significantly lower after PLS than after sham surgery, which is similar to a previous report of patients who underwent total knee arthroplasty [63]. To our knowledge, no data on the measurement of patella baja in rats is currently available, and so the findings from the present study may provide a reference.

This study has two main limitations. First, the rat model was established by PLS using Kirschner wires, which would inevitably cause damage to the infrapatellar fat pad and synovium

and change the walking pattern, as shown by limping and limb withdrawal. The effects of inflammatory factors in the synovial fluid and gait changes on the progression of PFJOA were not evaluated in this study. Second, although the mechanical properties of cartilage and intra-articular pressure were factors that cannot be ignored in this animal model, they were not fully investigated in this study due to the limitations of a study that included small numbers of patients. Further studies are needed to assess these complex factors in the progression of PFJOA.

Conclusions

A rat model of patellofemoral joint osteoarthritis (PFJOA) was developed using patellar ligament shortening (PLS), and the model was confirmed by investigating the changes in cartilage and subchondral bone. The model was developed at a low

cost and during a short duration. The study describes the development of the animal model and the evaluation of the alterations in the cartilage, subchondral bone, and soft tissues and has demonstrated similarity with findings described clinically in PFJOA. It is hoped that this animal model may be useful for future studies of PFJOA.

Acknowledgments

The authors thank Zhanying Wei and Hong Xu for providing technical support during micro-computed tomography (micro-CT) analysis and immunohistochemical analysis, respectively.

Conflict of interest

None.

References:

- Murray CJ, Vos T, Lozano R et al: Disability-adjusted life years (DALYs) for 291 diseases and injuries in 21 regions, 1990–2010: A systematic analysis for the Global Burden of Disease Study 2010. *Lancet*, 2012; 380: 2197–223
- Lawrence RC, Felson DT, Helmick CG et al: Estimates of the prevalence of arthritis and other rheumatic conditions in the United States. Part II. *Arthritis Rheum*, 2008; 58: 26–35
- Kim YM, Joo YB: Patellofemoral osteoarthritis. *Knee Surg Relat Res*, 2012; 24: 193–200
- Davies AP, Vince AS, Shepstone L et al: The radiologic prevalence of patellofemoral osteoarthritis. *Clin Orthop Relat Res*, 2002; (402): 206–12
- Collins NJ, Hinman RS, Menz HB, Crossley KM: Immediate effects of foot orthoses on pain during functional tasks in people with patellofemoral osteoarthritis: A cross-over, proof-of-concept study. *Knee*, 2017; 24: 76–81
- Naruse K, Urabe K, Jiang SX et al: Osteoarthritic changes of the patellofemoral joint in STR/OrtCrlj mice are the earliest detectable changes and may be caused by internal tibial torsion. *Connect Tissue Res*, 2009; 50: 243–55
- Salo PT, Seeratten RA, Erwin WM, Bray RC: Evidence for a neuropathic contribution to the development of spontaneous knee osteoarthrosis in a mouse model. *Acta Orthop Scand*, 2002; 73: 77–84
- McCoy AM: Animal models of osteoarthritis: comparisons and key considerations. *Vet Pathol*, 2015; 52: 803–18
- Takahashi I, Matsuzaki T, Kuroki H, Hosono M: Induction of osteoarthritis by injecting monosodium iodoacetate into the patellofemoral joint of an experimental rat model. *PLoS One*, 2018; 13: e0196625
- Gerwin N, Bendele AM, Glasson S, Carlson CS: The OARSI histopathology initiative – recommendations for histological assessments of osteoarthritis in the rat. *Osteoarthritis Cartilage*, 2010; 18(Suppl. 3): S24–34
- Malfait AM, Little CB, McDougall JJ: A commentary on modelling osteoarthritis pain in small animals. *Osteoarthritis Cartilage*, 2013; 21: 1316–26
- Clark AL, Leonard TR, Barclay LD et al: Heterogeneity in patellofemoral cartilage adaptation to anterior cruciate ligament transection: Chondrocyte shape and deformation with compression. *Osteoarthritis Cartilage*, 2006; 14: 120–30
- Chang NJ, Shie MY, Lee KW et al: Can early rehabilitation prevent posttraumatic osteoarthritis in the patellofemoral joint after anterior cruciate ligament rupture? Understanding the pathological features. *Int J Mol Sci* 2017; 18: pii: E829
- Clark AL, Leonard TR, Barclay LD et al: Opposing cartilages in the patellofemoral joint adapt differently to long-term cruciate deficiency: Chondrocyte deformation and reorientation with compression. *Osteoarthritis Cartilage*, 2005; 13: 1100–14
- Kilkenny C, Browne WJ, Cuthill IC et al: Improving bioscience research reporting: The ARRIVE guidelines for reporting animal research. *Osteoarthritis Cartilage*, 2012; 20: 256–60
- Grelsamer RP, Meadows S: The modified Insall-Salvati ratio for assessment of patellar height. *Clin Orthop Relat Res*, 1992; (282): 170–76
- Guingamp C, Gegout-Pottie P, Philippe L et al: Mono-iodoacetate-induced experimental osteoarthritis: A dose-response study of loss of mobility, morphology, and biochemistry. *Arthritis Rheum*, 1997; 40: 1670–79
- Aulin C, Lundback P, Palmblad K et al: An *in vivo* cross-linkable hyaluronan gel with inherent anti-inflammatory properties reduces OA cartilage destruction in female mice subjected to cruciate ligament transection. *Osteoarthritis Cartilage*, 2017; 25: 157–65
- Pritzker KP, Gay S, Jimenez SA et al: Osteoarthritis cartilage histopathology: Grading and staging. *Osteoarthritis Cartilage*, 2006; 14: 13–29
- Dai MW, Chu JG, Tian FM et al: Parathyroid hormone(1–34) exhibits more comprehensive effects than celecoxib in cartilage metabolism and maintaining subchondral bone micro-architecture in meniscectomized guinea pigs. *Osteoarthritis Cartilage*, 2016; 24: 1103–12
- Gou Y, Tian F, Kong Q et al: Salmon calcitonin attenuates degenerative changes in cartilage and subchondral bone in lumbar facet joint in an experimental rat model. *Med Sci Monit*, 2018; 24: 2849–57
- Iijima H, Aoyama T, Ito A et al: Effects of short-term gentle treadmill walking on subchondral bone in a rat model of instability-induced osteoarthritis. *Osteoarthritis Cartilage*, 2015; 23: 1563–74
- Tsai PH, Lee HS, Siow TY et al: Abnormal perfusion in patellofemoral subchondral bone marrow in the rat anterior cruciate ligament transection model of post-traumatic osteoarthritis: A dynamic contrast-enhanced magnetic resonance imaging study. *Osteoarthritis Cartilage*, 2016; 24: 129–33
- Egloff C, Sawatsky A, Leonard T et al: Effect of muscle weakness and joint inflammation on the onset and progression of osteoarthritis in the rabbit knee. *Osteoarthritis Cartilage*, 2014; 22: 1886–93
- Sawatsky A, Bourne D, Horisberger M et al: Changes in patellofemoral joint contact pressures caused by vastus medialis muscle weakness. *Clin Biomech (Bristol, Avon)*, 2012; 27: 595–601
- Chia WT, Pan RY, Tseng FJ et al: Experimental osteoarthritis induced by surgical realignment of the patella in BALB/c mice. *J Bone Joint Surg Br*, 2010; 92: 1710–16
- Arzi B, Wisner ER, Huey DJ et al: A proposed model of naturally occurring osteoarthritis in the domestic rabbit. *Lab Anim (NY)*, 2011; 41: 20–25
- Cook JL, Hung CT, Kuroki K et al: Animal models of cartilage repair. *Bone Joint Res*, 2014; 3: 89–94
- Teeple E, Jay GD, Elsaid KA, Fleming BC: Animal models of osteoarthritis: Challenges of model selection and analysis. *AAPS J*, 2013; 15: 438–46
- Mori Y, Kuroki Y, Yamamoto R et al: Clinical and histological study of patellar chondropathy in adolescents. *Arthroscopy*, 1991; 7: 182–97
- Meacham G, Emery IH: Quantitative aspects of patello-femoral cartilage fibrillation in Liverpool necropsies. *Ann Rheum Dis*, 1974; 33: 39–47

32. Bentley G: Articular cartilage changes in chondromalacia patellae. *J Bone Joint Surg Br*, 1985; 67: 769–74
33. Muellner T, Menth-Chiari WA, Funovics M et al: Shortening of the patellar tendon length does not influence the patellofemoral alignment in a cadaveric model. *Arch Orthop Trauma Surg*, 2003; 123: 451–54
34. Bertollo N, Pelletier MH, Walsh WR: Relationship between patellar tendon shortening and *in vitro* kinematics in the ovine stifle joint. *Proc Inst Mech Eng H*, 2013; 227: 438–47
35. Upadhyay N, Vollans SR, Seedhom BB, Soames RW: Effect of patellar tendon shortening on tracking of the patella. *Am J Sports Med*, 2005; 33: 1565–74
36. Bondeson J, Blom AB, Wainwright S et al: The role of synovial macrophages and macrophage-produced mediators in driving inflammatory and destructive responses in osteoarthritis. *Arthritis Rheum*, 2010; 62: 647–57
37. Clockaerts S, Bastiaansen-Jenniskens YM, Runhaar J et al: The infrapatellar fat pad should be considered as an active osteoarthritic joint tissue: A narrative review. *Osteoarthritis Cartilage*, 2010; 18: 876–82
38. Zhang Z, Leong DJ, Xu L et al: Curcumin slows osteoarthritis progression and relieves osteoarthritis-associated pain symptoms in a post-traumatic osteoarthritis mouse model. *Arthritis Res Ther*, 2016; 18: 128
39. Heard BJ, Solbak NM, Chung M et al: The infrapatellar fat pad is affected by injury induced inflammation in the rabbit knee: Use of dexamethasone to mitigate damage. *Inflamm Res*, 2016; 65: 459–70
40. Zhang M, Egan B, Wang J: Epigenetic mechanisms underlying the aberrant catabolic and anabolic activities of osteoarthritic chondrocytes. *Int J Biochem Cell Biol*, 2015; 67: 101–9
41. Hao HQ, Zhang JF, He QQ, Wang Z: Catilage oligomeric matrix protein, C-terminal cross-linking telopeptide of type II collagen, and matrix metalloproteinase-3 as biomarkers for knee and hip osteoarthritis (OA) diagnosis: A systematic review and meta-analysis. *Osteoarthritis Cartilage*, 2018 [Epub ahead of print]
42. Akhtar N, Khan NM, Ashruf OS, Haqqi TM: Inhibition of cartilage degradation and suppression of PGE2 and MMPs expression by pomegranate fruit extract in a model of posttraumatic osteoarthritis. *Nutrition*, 2017; 33: 1–13
43. Zhang Q, Lai S, Hou X et al: Protective effects of PI3K/Akt signal pathway induced cell autophagy in rat knee joint cartilage injury. *Am J Transl Res*, 2018; 10: 762–70
44. Darnell JE Jr, Kerr IM, Stark GR: Jak-STAT pathways and transcriptional activation in response to IFNs and other extracellular signaling proteins. *Science*, 1994; 264: 1415–21
45. Liu J, Cao L, Gao X et al: Ghrelin prevents articular cartilage matrix destruction in human chondrocytes. *Biomed Pharmacother*, 2018; 98: 651–55
46. Latourte A, Cherifi C, Maillet J et al: Systemic inhibition of IL-6/Stat3 signalling protects against experimental osteoarthritis. *Ann Rheum Dis*, 2017; 76: 748–55
47. Greene DA, Winegrad AI, Carpentier JL et al: Rabbit sciatic nerve fascicle and 'endoneurial' preparations for *in vitro* studies of peripheral nerve glucose metabolism. *J Neurochem*, 1979; 33: 1007–18
48. Legendre F, Bogdanowicz P, Boumediene K, Pujol JP: Role of interleukin 6 (IL-6)/IL-6R-induced signal transducers and activators of transcription and mitogen-activated protein kinase/extracellular. *J Rheumatol*, 2005; 32: 1307–16
49. Burr DB, Gallant MA: Bone remodelling in osteoarthritis. *Nat Rev Rheumatol*, 2012; 8: 665–73
50. Hayami T, Pickarski M, Zhuo Y et al: Characterization of articular cartilage and subchondral bone changes in the rat anterior cruciate ligament transection and meniscectomized models of osteoarthritis. *Bone*, 2006; 38: 234–43
51. Bellido M, Lugo L, Roman-Blas JA et al: Subchondral bone microstructural damage by increased remodelling aggravates experimental osteoarthritis preceded by osteoporosis. *Arthritis Res Ther*, 2010; 12: R152
52. Kihara S, Hayashi S, Hashimoto S et al: Cyclin-dependent kinase inhibitor-1-deficient mice are susceptible to osteoarthritis associated with enhanced inflammation. *J Bone Miner Res*, 2017; 32: 991–1001
53. Liu YD, Liao LF, Zhang HY et al: Reducing dietary loading decreases mouse temporomandibular joint degradation induced by anterior crossbite prosthesis. *Osteoarthritis Cartilage*, 2014; 22: 302–12
54. Yang X, He H, Gao Q, He C: Pulsed electromagnetic field improves subchondral bone microstructure in knee osteoarthritis rats through a Wnt/beta-catenin signaling-associated mechanism. *Bioelectromagnetics*, 2018; 39: 89–97
55. Romas E, Gillespie MT, Martin TJ: Involvement of receptor activator of NFkappaB ligand and tumor necrosis factor-alpha in bone destruction in rheumatoid arthritis. *Bone*, 2002; 30: 340–46
56. Goldring SR, Goldring MB: Bone and cartilage in osteoarthritis: Is what's best for one good or bad for the other? *Arthritis Res Ther*, 2010; 12: 143
57. Henak CR, Kapron AL, Anderson AE et al: Specimen-specific predictions of contact stress under physiological loading in the human hip: Validation and sensitivity studies. *Biomech Model Mechanobiol*, 2014; 13: 387–400
58. Wluka AE, Wang Y, Davis SR, Cicuttini FM: Tibial plateau size is related to grade of joint space narrowing and osteophytes in healthy women and in women with osteoarthritis. *Ann Rheum Dis*, 2005; 64: 1033–37
59. van Bussel CM, Stronks DL, Huygen FJ: Complex regional pain syndrome type I of the knee: A systematic literature review. *Eur J Pain*, 2014; 18: 766–73
60. Otsuki S, Murakami T, Okamoto Y et al: Risk of patella baja after opening-wedge high tibial osteotomy. *J Orthop Surg (Hong Kong)*, 2018; 26: 2309499018802484
61. Wyndow N, Collins N, Vicenzino B et al: Is there a biomechanical link between patellofemoral pain and osteoarthritis? A narrative review. *Sports Med*, 2016; 46: 1797–808
62. Phillips CL, Silver DA, Schranz PJ, Mandalia V: The measurement of patellar height: A review of the methods of imaging. *J Bone Joint Surg Br*, 2010; 92: 1045–53
63. Xu B, Xu WX, Lu D et al: Application of different patella height indices in patients undergoing total knee arthroplasty. *J Orthop Surg, Res* 2017; 12: 191